IOP Publishing Journal of Physics A: Mathematical and Theoretical
J. Phys. A: Math. Theor. **49** (2016) 285202 (17pp) doi:10.1088/1751-8113/49/28/285202

On the divergence of gradient expansions for kinetic energy functionals in the potential functional theory

Alexey Sergeev[1], **Raka Jovanovic**[1], **Sabre Kais**[1,2] and **Fahhad H Alharbi**[1,2]

[1] Qatar Environment and Energy Research Institute (QEERI), Hamad Bin Khalifa University (HBKU), Doha, Qatar
[2] College of Science and Engineering, Hamad Bin Khalifa University (HBKU), Doha, Qatar

E-mail: asergeev@qf.org.qa

Received 3 September 2015, revised 7 December 2015
Accepted for publication 19 May 2016
Published 6 June 2016

Abstract

We consider the density of a fermionic system as a functional of the potential, in one-dimensional case, where it is approximated by the Thomas–Fermi term plus semiclassical corrections through the gradient expansion. We compare this asymptotic series with the exact answer for the case of the harmonic oscillator and the Morse potential. It is found that the leading (Thomas–Fermi) term is in agreement with the exact density, but the subdominant term does not agree in terms of the asymptotic behavior because of the presence of oscillations in the exact density, but their absence in the gradient expansion. However, after regularization of the density by convolution with a Gaussian, the agreement can be established even in the subdominant term. Moreover, it is found that the expansion is always divergent, and its terms grow proportionally to the factorial function of the order, similar to the well-known divergence of perturbation series in field theory and the quantum anharmonic oscillator. Padé–Hermite approximants allow summation of the series, and one of the branches of the approximants agrees with the density.

Keywords: potential functional theory, density functional theory, gradient expansion, Padé approximants

(Some figures may appear in colour only in the online journal)

1. Introduction

Finding the kinetic energy of a non-interacting fermionic system as a functional of its electron density, or alternatively the density as a functional of the potential (known as potential functional approximation) [1–4] is at the core of the modern orbital–free density functional theory, which allows one to save computation time in comparison with the traditional Kohn–Sham approach based on decomposition over a set of one-electron orbitals. The Thomas–Fermi approximation, which is a local density approximation, is the earliest known result and probably the most fundamental one.

Since the introduction of potential functional approximations (PFA) and the establishment of their duality to the density functional theory (DFT) [5, 6], there have been few dedicated attempts to develop potential functionals. The initial routes are based on corrections to the Thomas–Fermi limit. Yang and coworkers [5, 7] applied the gradient expansion approach, while Burke and his team opted to develop a non-gradient based expansion [8]. Actually, the origin of PFA can be traced back even earlier. Holas and March used the microscopic virial theorem to develop a differential operation that connects the non-interacting kinetic energy to a source that depends only on the density, the potential, and their derivatives [5]. Also, many authors tried to refine the Thomas–Fermi model for N-body problems in ways that can be connected to PFA [6–13].

Semiclassical approximation for $\rho[v]$, where ρ is the electron density of the ground state of a system of N non-interacting electrons, is known as the gradient expansion [3]:

$$\rho[v] = \frac{p_{\mathrm{F}}^3}{3\pi^2}\left[1 - \frac{\nabla^2 v}{4p_{\mathrm{F}}^4} - \frac{(\nabla v)^2}{8p_{\mathrm{F}}^6} + \ldots\right], \tag{1}$$

where the Fermi momentum is defined as $p_{\mathrm{F}} = \sqrt{2(\mu - v)}$, and the chemical potential μ is defined implicitly by the equation

$$\int \rho(\boldsymbol{r})\mathrm{d}\boldsymbol{r} = N, \tag{2}$$

where the integration is performed over the classically allowed region $v(\boldsymbol{r}) < \mu$. The gradient expansion is known as the most systematic generalization of the Thomas–Fermi method, where each term is derived rigorously.

The gradient expansion for the kinetic energy density (in three-dimensional case) can be obtained too [3],

$$t[v] = \frac{p_{\mathrm{F}}^5}{10\pi^2}\left[1 - \frac{25\nabla^2 v}{12p_{\mathrm{F}}^4} + \frac{15(\nabla v)^2}{8p_{\mathrm{F}}^6} + \ldots\right]. \tag{3}$$

Equations (1) and (3), in the leading order, after elimination of p_{F}, give a well-known Thomas–Fermi local density approximation. Here, we focus mainly on the expansion given by equation (1).

Obviously, the expressions in square brackets in equations (1) and (3) have the form of formal power series in the parameter $\lambda = 1/p_{\mathrm{F}}^2$. In the limit of $\lambda \to 0$, the series is approximated by their respective leading terms equal to one, i.e. giving the Thomas–Fermi limits $\frac{p_{\mathrm{F}}^3}{3\pi^2}$ and $\frac{p_{\mathrm{F}}^5}{10\pi^2}$ for the electron and the kinetic energy densities respectively. Since the terms $\sim\lambda$ are missing, the next approximation starts from the second-order terms ($\sim\lambda^2$). Notice that all terms in equations (1) and (3) are finite except for the special case of a turning point ($p_{\mathrm{F}} = 0$). In contrast, the gradient expansion for the total kinetic energy $T_{\mathrm{s}}[\rho]$ of bound

systems gives infinite terms starting from the sixth-order gradient correction because of the divergent integrand for finite systems [14, 15].

The applicability of the gradient expansion depends on the starting point (the leading term). The Thomas–Fermi model assumes that the density is uniform and extended to infinity. So, the conventional gradient expansion is valid for a small variation from that case. Examples of this are metals. For finite systems, the Thomas–Fermi model is not a good starting point. Such an application has two main shortcomings. The first is the problem of the divergence. The second is the need for huge numbers of expansion corrections to account for the severe difference from the uniform density assumed by the Thomas–Fermi model. This makes such an expansion impractical.

It should be noted that the accuracy of the gradient expansion deteriorates in regions of small Fermi momenta p_{F} when the denominators in equations (1) and (3) become small, and that the gradient expansion completely breaks up at turning points ($p_{\mathrm{F}} = 0$). Because of these limitations, there is a tendency to avoid the gradient expansion altogether by developing alternative approaches based for example on a uniform semiclassical approximation [16] or exactly solvable models [13]. We try to revive interest in the gradient expansion by considering higher orders of the expansion and by applying the averaging at low orders.

The purpose of this study is to assess the asymptotic behavior of the series (1) as well as its convergence. However, a practical algorithm of calculation of the gradient expansion for three-dimensional potentials beyond the first few terms remains to be developed [17]. In order to calculate a large number of terms of the series, we consider the case of a one-dimensional potential $v\,(x)$. Then, the higher-order terms can be easily calculated by recurrence relations, and since the gradients reduce to multiple derivatives, the gradient expansion has an especially compact form [17]:

$$\rho[v] = \frac{p_{\mathrm{F}}}{\pi}\left[1 + \frac{v''}{12p_{\mathrm{F}}^4} + \frac{10v'^2 - v''''}{80p_{\mathrm{F}}^6} + \ldots\right]. \tag{4}$$

The paper is organized as follows. In section 2, we derive higher orders of the gradient expansion for two benchmark cases of the harmonic and Morse potentials, in one dimension. In section 3, we study the accuracy of the leading term (Thomas–Fermi approximation) and highlight the difficulties of using the gradient expansion in the second-order (i.e. the leading term plus the term $\sim\lambda^2$). In section 4, we determine the radius of convergence of series (1) and (3) and study the asymptotic growth of the coefficients of the series at large orders.

In section 5, we consider a problem of restoration of the function $\rho[v]$ from its divergent asymptotic series given by the gradient expansion. Here, we use generalized summation methods that allow one to extend analytically a function expanded into a power series beyond its radius of convergence. Using Padé approximants and more generalized Padé–Hermite approximants, it is shown that the result of summation consists of a multiple-valued analytic function whose main branch is close to the Thomas–Fermi approximation and does not have oscillations, while its secondary branch coincides with the oscillating function $\rho[v]$. These numerical coincidences and regularities invite further theoretical studies and possibly a rigorous proof.

Table 1. Coefficients of the gradient expansion (5) for the harmonic oscillator $v = x^2/2$.

n	b_n
0	1
1	0
2	$\frac{1}{12}$
3	$\frac{1}{8}x^2$
4	$-\frac{3}{32}$
5	$-\frac{77}{96}x^2$
6	$\frac{61}{128} - \frac{105}{128}x^4$
7	$\frac{2739}{256}x^2$
8	$\frac{17017}{512}x^4 - \frac{180323}{30720}$
9	$\frac{25025}{1024}x^6 - \frac{259259}{1024}x^2$
10	$\frac{1099917}{8192} - \frac{6512649}{4096}x^4$
11	$\frac{154829727}{16384}x^2 - \frac{37182145}{12288}x^6$
12	$-\frac{56581525}{32768}x^8 + \frac{1632457827}{16384}x^4 - \frac{322885335}{65536}$
13	$\frac{11444664231}{32768}x^6 - \frac{168084074313}{327680}x^2$
14	$\frac{188699385875}{393216}x^8 - \frac{6411413356465}{786432}x^4 + \frac{624803155685}{2359296}$

2. Calculation of higher orders of the gradient expansion for two examples of one-dimensional potentials

Let us denote by b_n the coefficients of the series in equation (4), so that

$$\rho[v] = \frac{p_F}{\pi}\sum_{n=0}^{\infty} b_n \lambda^n, \qquad \lambda = \frac{1}{p_F^2}. \tag{5}$$

Samaj and Percus [17] give a recursive algorithm for calculation of the coefficients b_n. First, define $a_0 = 1$. Then, for each $n = 1, 2, 3, \ldots$ calculate

$$\begin{aligned} a_n = &-\frac{1}{2}\sum_{r=1}^{n-1} a_r a_{n-r} + \frac{1}{8}\sum_{r=0}^{n-1}(a_r' a_{n-r-1}' - 2a_r a_{n-r-1}'') \\ &-\frac{1}{2}\sum_{r=0}^{n-2}[(n-r-3/2)v'' a_r a_{n-r-2} + (2n-3r-7/2)v' a_r a_{n-r-2}'] \\ &+\frac{1}{2}\sum_{r=0}^{n-3}(n-r-5/2)(2n-3r-7/2)v'^2 a_r a_{n-r-3}, \end{aligned} \tag{6}$$

where the prime indicates a derivative with respect to the coordinate x, and the double prime indicates the second derivative. Finally, calculate

$$b_n = \frac{a_n}{1-2n}. \tag{7}$$

For the details, we refer the reader to the paper [17].

For cases of a harmonic oscillator and a Morse potential, the coefficients of the series (5) have an especially simple form of polynomial expressions. The first 15 coefficients b_n for the

Table 2. Coefficients of the gradient expansion (5) for the Morse potential $v(x) = 15(\mathrm{e}^{-x/2} - 2\mathrm{e}^{-x/4})$. Here, $t = \mathrm{e}^{-x/4}$.

n	b_n
0	1
1	0
2	$\frac{5}{16}t^2 - \frac{5}{32}t$
3	$\frac{225}{32}t^4 - \frac{225}{16}t^3 + \frac{1797}{256}t^2 + \frac{3}{2048}t$
4	$-\frac{1575}{512}t^4 + \frac{225}{64}t^3 - \frac{22035}{28672}t^2 - \frac{15}{917504}t$
5	$-\frac{86625}{512}t^6 + \frac{433125}{1024}t^5 - \frac{2766075}{8192}t^4 + \frac{5511375}{65536}t^3 + \frac{17765}{393216}t^2 + \frac{5}{25165824}t$
6	$-\frac{5315625}{2048}t^8 + \frac{5315625}{512}t^7 - \frac{63122625}{4096}t^6 + \frac{661435875}{65536}t^5 - \frac{320496975}{131072}t^4 - \frac{42417225}{2097152}t^3 - \frac{225105}{92274688}t^2 - \frac{15}{5905580032}t$

harmonic oscillator $v = x^2/2$ are listed in table 1. To study the behavior of the coefficients b_n at large orders, we used recurrence relations (6)–(7) to calculate higher-order b_n up to $n = 3500$.

Our second example is the Morse potential

$$v(x) = D(e^{-2ax} - 2e^{-ax}). \tag{8}$$

We consider here the same parameters $a = 1/4$ and $D = 15$ as in the paper [16] where the Morse potential was used as a benchmark test for the uniform semiclassical approximation. The first 7 coefficients b_n are listed in table 2. Due to the fact that the Morse potential needs higher order polynomials in comparison with the harmonic oscillator, we are able to calculate here fewer terms of the series, up to $n = 1450$.

3. Asymptotic behavior of the gradient expansion at lower orders

Let us compare the leading term of the expansion with the exact density. The leading term is given by equation $\rho_{\mathrm{TF}}(x) = p_{\mathrm{F}}(x)/\pi$, where $p_{\mathrm{F}}(x) = \sqrt{2(\mu - v(x))}$. There, the chemical potential μ is determined from the normalization condition $\int \rho_{\mathrm{TF}}(x)\mathrm{d}x = N$. We find that the chemical potential $\mu = N$ in case of the harmonic oscillator and $\mu = -D + a\sqrt{2D}\left(N - \frac{a}{2\sqrt{2D}}N^2\right)$ in case of the Morse potential. Note that while N can be arbitrarily large for the harmonic oscillator, it is limited by the number of bound states for the Morse potential: $N < \frac{\sqrt{2D}}{a}$ (for our parameters $a = 1/4$ and $D = 15$, $N \leqslant 21$).

The exact density is

$$\rho(x) = \sum_{n=0}^{N-1} \psi_n^2(x), \tag{9}$$

where the wavefunctions are

$$\psi_n(x) = (\pi^{1/2}2^n n!)^{-1/2} H_n(x)\mathrm{e}^{-x^2/2}$$

for the harmonic oscillator and

$$\psi_n(x) = \mathcal{N} z^{\beta - n - 1/2} L_n^{2\beta - 2n - 1}(z)\mathrm{e}^{-z/2}$$

where

$$z = 2\beta \mathrm{e}^{-ax}, \quad \beta = \sqrt{2D}/a, \quad \mathcal{N} = \sqrt{a\frac{2\beta - 2n - 1}{\Gamma(2\beta - n)}n!}$$

Table 3. Convergence of Padé approximants (PA), quadratic Padé approximants (QPA) and cubic Padé approximants (CPA) for the harmonic oscillator at $N = 1$ and $x = 1$. n is the order of the approximants as defined in the paper. Exact density is 0.207554 and the Thomas–Fermi approximation is 0.31831.

n	PA	QPA	CPA
5	0.33847	0.35146, 0.26541	0.35231, 0.35285 ± 0.03353 i
6	0.36455	0.35364, 0.18341	0.35163, 0.32810 ± 0.07451 i
7	0.36516	0.34924, 0.33511	0.35154, 0.33482, 0.27916
8	0.36456	0.35184, 0.22463	0.34199, 0.35344, 0.25253
9	0.33375	0.37998 ± 0.00727 i	0.34882, 0.36514, 0.45203
10	0.35819	0.34211, 0.39576	0.35123, 0.37754, 0.23459
20	0.35460	0.34747, 0.29446	0.34910 ± 0.00493 i, 0.26036
50	0.33014	0.34255, 0.22857	0.34312, 0.30398, 0.24986
100	0.29831	0.34343, 0.18316	0.34335, 0.27484, 0.22093
200	0.30829	0.34339, 0.16870	0.34338, 0.21594 ± 0.04745 i
500	0.24166	0.34338, 0.62228 i	0.34338, 0.20643 ± 0.07366 i
1000	0.18353	0.34338, 0.25911	0.34338, 0.20757 ± 0.07336 i
1500	0.12518	0.34338, 0.11088 i	0.34338, 0.20755 ± 0.07343 i
2000	0.13363	0.34338, 0.26875	0.34338, 0.20755 ± 0.07343 i
2500	0.11364	0.34338, 0.21285	0.34338, 0.20755 ± 0.07343 i
3000	0.11774 i	0.34338, 0.56909 i	0.34338, 0.20755 ± 0.07343 i
3498	0.32389 i	0.34338, 0.13792	0.34338, 0.20755 ± 0.07343 i

for the Morse potential. Here, $H_n(x)$ is the Hermite polynomial and $L_n^{\alpha}(z)$ is the generalized Laguerre polynomial.

Figure 1 shows the electron density versus the coordinate. The density oscillates around its Thomas–Fermi limit, and the amplitude of oscillation decreases as the number of particles increases. The Thomas–Fermi density vanishes at turning points x_1, x_2 given by equation $v(x_{1,2}) = \mu$. For both potentials, the correction to the Thomas–Fermi density, $\delta\rho(x) = \rho(x) - \rho_{\mathrm{TF}}(x)$ is an oscillating function on the interval (x_1, x_2) that has $2(N + 1)$ sign changes.

We show below that these oscillations are subdominant with respect to the leading term of the gradient expansion (4), i.e. the Thomas–Fermi density. However, these oscillations are much larger in comparison to the next non-zero term of the gradient expansion. This confirms the known fact [18, 19] that the oscillations cannot be accounted for by adding corrections to the Thomas–Fermi limit. Alternatively, we consider a modified density with artificially suppressed oscillations and compare this function with the gradient expansion. We found that after removing the oscillations by a convolution with a Gaussian function, the correction to the Thomas–Fermi density $\delta\rho$ asymptotically matches with the correction found from the gradient expansion. It is a new result that is demonstrated here numerically.

Let us focus on the asymptotic series $F(\lambda)$ in the square brackets in equation (4),

$$\frac{\rho(x)}{\rho_{\mathrm{TF}}(x)} = F(\lambda) \sim 1 + b_2(x)\lambda^2 + b_3(x)\lambda^3 + \ldots, \tag{10}$$

with $\lambda = 1/p_{\mathrm{F}}^2$ and the coefficients b_n defined through gradients of the potential. We are going to verify equation (10) numerically for the case of the harmonic oscillator, $v(x) = x^2/2$. More specifically, we are going to compare both sides of equation (10) for progressively decreasing values of the parameter λ. Recalling that $p_{\mathrm{F}} = \sqrt{2(\mu - v)}$ and that μ accepts discrete values $\mu = N = 1, 2, 3, \ldots$, we see that the small parameter λ is discretized too, $\lambda = \frac{1}{2}(N - v)^{-1}$,

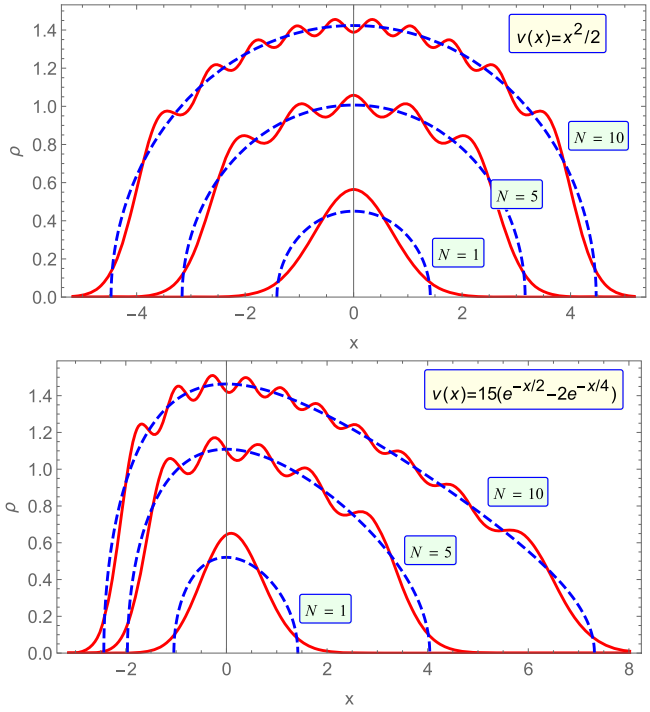

Figure 1. Thomas–Fermi density (dashed curves) and exact density (solid curves) for $N = 1$, 5, and 10 particles. The upper panel refers to the harmonic oscillator, and the lower panel to the Morse potential.

where N is a positive integer. In order to allow the comparison for continuously changing parameter λ, we performed an interpolation according to the uniform semiclassical approximation ρ_{sc} developed by Ribeiro *et al* [16]. For the harmonic oscillator, we found after performing integrations that

$$\rho_{sc} = \frac{p}{6}\left[3^{4/3} q\ \mathrm{Ai}^2(s) + \left(\frac{12\mu}{p^3} - \frac{8}{q^3}\right)\mathrm{Ai}(s)\mathrm{Ai}'(s) + \frac{4\cdot 3^{2/3}}{q}\mathrm{Ai}'^2(s)\right], \tag{11}$$

where

$$s = -\frac{3^{2/3}}{4}q^2, \quad q = 2^{1/3}\left[\mu\left(\pi + 2\arcsin\frac{x}{\sqrt{2\mu}}\right) + px\right]^{1/3}. \tag{12}$$

In equations (11) and (12), the momentum p is expressed through λ as $p = \lambda^{-1/2}$, and $\mu = p^2/2 + x^2/2$. The equations are valid for the classically allowed region $p > 0$, but they could in principle be analytically extended to the classically forbidden, or evanescent region $p < 0$. They are valid for $x \leqslant 0$. Similar formulas for positive coordinates exist too.

To verify equation (10) in the zero order, we are going to show numerically that

$$\frac{\rho(x)}{\rho_{\mathrm{TF}}(x)} \to 1 \tag{13}$$

as $\lambda \to 0$. Figure 2 shows this ratio as a function of λ for two different values of the coordinate x. As the oscillations are damped out for small λ, this clearly verifies equation (13). This is the case for all other coordinates as well.

To verify equation (10) in the second order, we need to show that

$$\frac{1}{b_2\lambda^2}\left[\frac{\rho(x)}{\rho_{\mathrm{TF}}(x)} - 1\right] \to 1 \tag{14}$$

as $\lambda \to 0$. Figure 3 shows λ-dependence of the lhs of equation (14) for two different values of the coordinate x. Here, we plot this value versus λ^{-1} instead of λ in order to make a period of oscillations of the function constant. Obviously, the function does not approach any limit as $\lambda^{-1} \to \infty$.

To suppress the oscillations without losing the trend of the function as λ^{-1} increases, we suggest considering a convolution of this oscillating function with a Gaussian $g(t) = \frac{1}{\sqrt{\pi}T}\mathrm{e}^{-t^2/T^2}$, i.e.

$$\tilde{f}(t) = \int_0^\infty f(t')g(t - t')\mathrm{d}t', \tag{15}$$

where the function f is defined as

$$f(\lambda^{-1}) = \frac{1}{b_2\lambda^2}\left[\frac{\rho(x)}{\rho_{\mathrm{TF}}(x)} - 1\right]. \tag{16}$$

This convolution is known as a low-pass filter removing high frequency Fourier components with a period of oscillations smaller than the constant T. Figure 4 shows the results for the case of the harmonic oscillator. There, the parameter $T = 50$ is chosen such that $T \gg T_0$, where T_0 is the period of oscillations of the function f, which is around 3.6. The figure shows that after smoothing the oscillations of the function f, the transformed function g goes to the correct limit, equal to that predicted by the gradient expansion in the second order. In the above tests, we use the same value of the chemical potential as in the Thomas–Fermi limit, i.e. $\mu = N$.

In a similar study of effects of averaging, Alonso and Girifalco [20] found that the inclusion of gradient terms gives substantial improvement for the energy of atoms by cancellation of errors of the energy density in different regions. Thus, the success of the gradient expansion for atoms can be attributed to averaging of the local kinetic energy density over the atomic shell structure [21].

4. Zero radius of convergence of the gradient expansion and growth of its terms at large orders

Here, we determine the behavior of the coefficients of the gradient expansion for the electron density and for the kinetic energy density,

$$\rho[v] = \frac{p_{\mathrm{F}}}{\pi}\sum_{n=0}^{\infty} b_n\lambda^n, \quad t[v] = \frac{p_{\mathrm{F}}^3}{2\pi}\sum_{n=0}^{\infty} c_n\lambda^n \tag{17}$$

at large orders n. These coefficients are expressed through the coefficients a_n that can be calculated by recurrence relations (6) as $b_n = \frac{1}{1-2n}a_n$ and $c_n = \frac{1}{3-2n}a_n$ [17]. Therefore, at large n we have $b_n \sim c_n \sim -\frac{1}{2}n^{-1}a_n$, and so for our purpose it is sufficient to determine large-order behavior of the coefficients a_n only.

We show numerical evidence that the radius of convergence of the gradient expansion is zero. For the harmonic oscillator, we show that the coefficients grow as $n!$, and for the Morse potential even faster as $\left(\frac{5}{3}n\right)!$. These results may be of interest in relation to applicability of

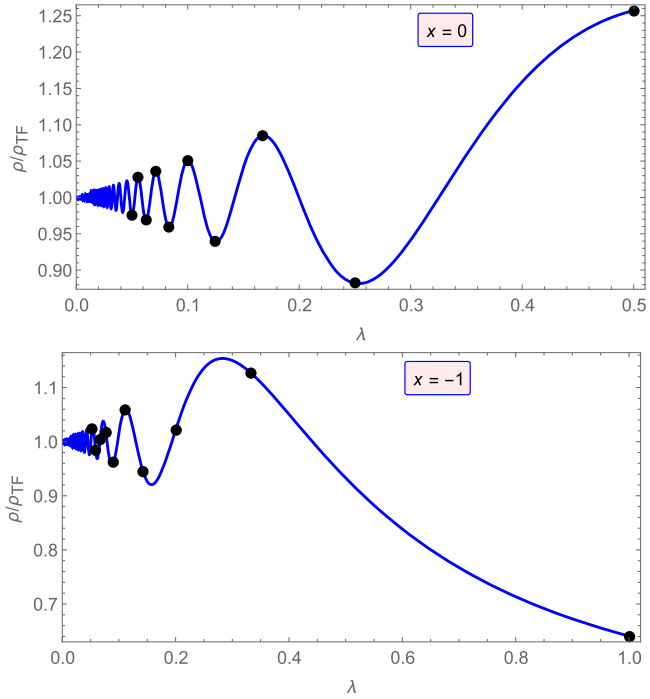

Figure 2. Ratio of the density to the Thomas–Fermi density as the parameter λ goes to zero. Dots are cases when $\int \rho_{\rm TF}\, d\boldsymbol{r} = N$ where N is a positive integer $1, 2, \ldots, 10$. Curves are calculated for continuous values of λ using accurate semiclassical approximation $\rho_{\rm sc}$ for the density given by equations (11) and (12). Upper panel is the case of $x = 0$, and lower panel $x = -1$. Notice that for small parameters λ, the oscillation amplitude decreases proportional to λ, but the correction to the Thomas–Fermi is of the order $\sim\lambda^2$, see equation (10).

generalized summation methods such as Padé approximants. For example, for the class of Stieltjes functions, Padé approximants converge for the series growing as $n!$, but may diverge for the series growing as $(3n)!$ [22]. Particularly, the Stieltjes theory predicts convergence of Padé approximants for eigenvalue perturbation series of the quantum anharmonic oscillator $x^2 + \lambda x^4$ [22, 23], but the evidence was found to be against the convergence in the case of the octic anharmonic oscillator $x^2 + \lambda x^8$ when the series grows as $(3n)!$ [24].

Let us start from the harmonic oscillator, and from the case of $x = 0$. Firstly, we notice that all odd-order coefficients vanish, and even-order coefficients have alternating signs. Further we note that the ratio $a_{2n}/a_{2(n+1)}$ goes to zero at large n, and so the radius of convergence of the series is zero. We consider here the Borel transform of the series [22],

$$\tilde{a}_n = a_n/n!. \tag{18}$$

Calculating the ratio for this new series,

$$r_n = \left| \frac{\tilde{a}_{2n}}{\tilde{a}_{2(n+1)}} \right|^{1/2}, \tag{19}$$

we can see that it tends to $2/\pi$ as $n \to \infty$. Now, assuming that the large order behavior of the coefficients has the form which is typical in many quantum-mechanical problems [25, 26],

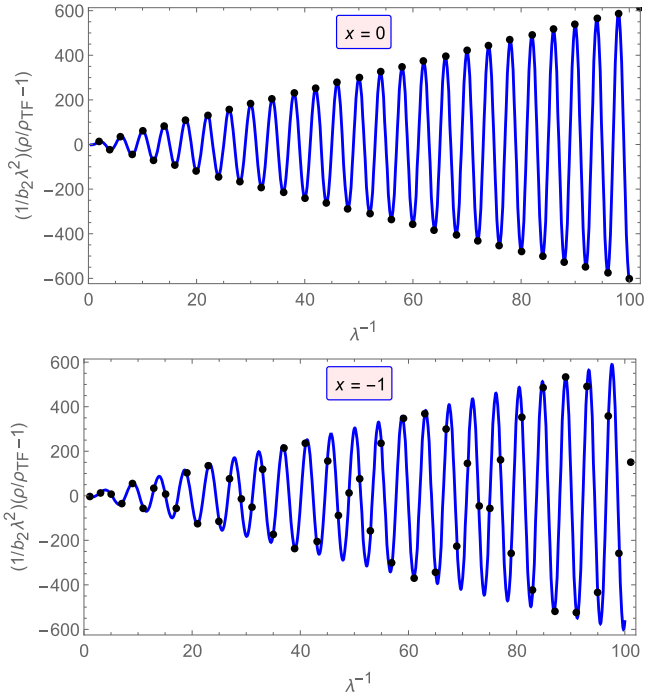

Figure 3. L.h.s. of equation (14) versus λ^{-1}. Dots are cases when $\int \rho_{\mathrm{TF}}\, \mathrm{d}\boldsymbol{r} = N$ where N is a positive integer $1, 2, \ldots, 100$. Upper panel is the case of $x = 0$, and lower panel $x = -1$. Notice that the oscillations don't damp out in the limit of $\lambda \to 0$, or alternatively $\lambda^{-1} \to \infty$.

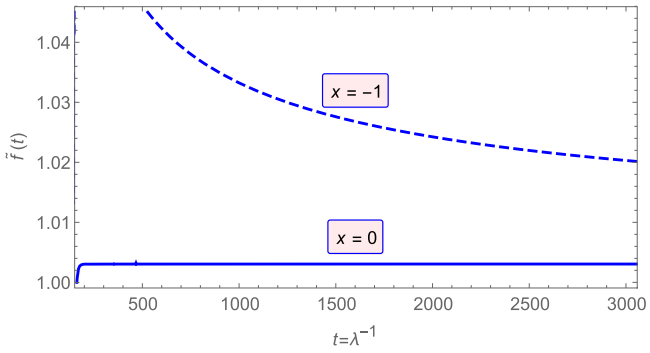

Figure 4. The same function as shown on figure 3 but after a convolution with the Gaussian $\frac{1}{50\sqrt{\pi}}\mathrm{e}^{-t^2/2500}$. The result of the convolution $\tilde{f}(t)$ given by equation (15) is plotted versus the parameter $t = \lambda^{-1}$. Rapidly increasing oscillations of the original function $f(t)$ are completely suppressed by the averaging. The smoothed function $\tilde{f}(t)$ converges to the limit equal to one at large t. Thus, the validity of the second gradient correction for the averaged values is validated.

$$a_n \sim (n+\beta)!(CA^n + C^\star A^{\star n}), \tag{20}$$

we can see that $A = \frac{\pi}{2}\mathrm{i}$ from the fact that $r_n \to \pi/2$ together with $a_{2n+1} = 0$, and $\mathrm{sign}(a_{2n}) = (-1)^n$.

Further numerical studies allow us to determine the remaining two parameters, $\beta = -1$ and $C = 1/\pi$. So finally we obtain $a_n \sim A_n$, where the asymptotic limit of the coefficients a_n is

$$A_n = \frac{2}{\pi}(n-1)!\left(\frac{\pi}{2}\mathrm{i}\right)^n \tag{21}$$

if n is even and zero if n is odd. Numerically, we found that the ratio a_n/A_n rapidly approaches the limit equal to one as n increases, see figure 5 below.

For small values of the coordinate x, we expand the coefficients a_n as follows,

$$a_n = a_n^{(0)} + a_n^{(2)}x^2 + a_n^{(4)}x^4 + \ldots, \tag{22}$$

where $a_n^{(0)} = a_n|_{x=0}$, $a_n^{(2)} = \frac{1}{2}\frac{\mathrm{d}}{\mathrm{d}x^2}a_n|_{x=0}$, and $a_n^{(4)} = \frac{1}{24}\frac{\mathrm{d}}{\mathrm{d}x^4}a_n|_{x=0}$. We already found that $a_n^{(0)} \sim A_n$. A similar analysis allows us to determine the large-order asymptotical behavior for corrections at small values of x, $a_n^{(2)} \sim -2A_{n+1}$ and $a_n^{(4)} \sim \frac{2}{3}A_{n+2}$. Figure 5 shows that the ratios $\frac{a_n^{(0)}}{A_n}$, $\frac{a_n^{(2)}}{-2A_{n+1}}$, and $\frac{a_n^{(4)}}{2/3A_{n+2}}$ tend to one as n increases.

Now, let us consider the case of non-zero coordinate x as well as the case of the Morse potential. We tried to estimate the radius of convergence R of the Borel transform, $\tilde{a}_n$, using the ratio test, i. e. calculating the ratios $|\tilde{a}_n/\tilde{a}_{n-1}|$ and estimating the large-n limit that should be equal to $1/R$. However, these ratios do not show certain convergence because of strong oscillations. A generalized ratio test was proposed by Mercer and Roberts [27]. Consider a sequence of ratios

$$r_n = \left(\frac{\tilde{a}_{n+1}\tilde{a}_{n-1} - \tilde{a}_n^2}{\tilde{a}_n\tilde{a}_{n-2} - \tilde{a}_{n-1}^2}\right)^{1/2}. \tag{23}$$

Then, in the large-n limit, $r_n \to \frac{1}{R}$. This ratio test shows that the radius of convergence is the same for all x and equal to $R = \pi/2$, see figure 6 (upper panel).

For the Morse potential, we found that the radius of convergence of the Borel transform is zero, i.e. the series diverges faster than the series of factorials. However, we found that the radius of convergence of the generalized Borel transform

$$\tilde{a}_n = a_n/\left(\frac{5}{3}n\right)! \tag{24}$$

is finite, i.e. in this case the series grows as $\left(\frac{5}{3}n\right)!$. The generalized ratio test is shown on figure 6 on the lower panel. Apparently, the inverse radius of convergence which is equal to the limit at $n \to \infty$ in this case grows as the coordinate x increases.

5. Use of generalized summation methods to recover the expanded function from its gradient expansion

Since the gradient expansion has zero radius of convergence, partial sums of the series are always divergent. In addition, the n-th term diverges as $1/(x - x_\mathrm{t})^{2n-1}$ at a turning point x_t where $v(x_\mathrm{t}) = 0$, and so the n-th partial sum diverges at turning points in a similar way.

There is an extensive discussion of how to 'sum' a divergent power series, i.e. how to reconstruct a function from its divergent Taylor expansion [28, 29]. An approximation that is

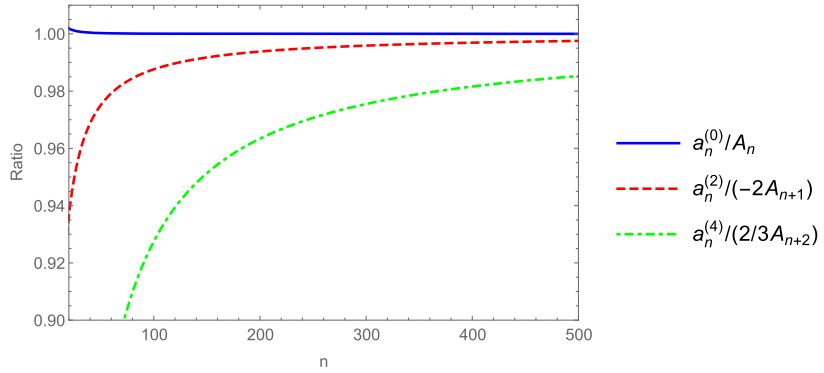

Figure 5. Ratio of the coefficients of gradient expansion at $x = 0$, $a_n^{(0)}$, and the corrections for small x given by equation (22) to their large-order asymptotical expressions, A_n, $-2A_{n+1}$, and $2/3A_{n+2}$, where A_n is defined by equation (21). The ratio $\frac{a_n^{(0)}}{A_n}$ rapidly approaches one as n increases. For the largest calculated order $n = 3500$, it is exceedingly close to one, $a_{3500}/A_{3500} = 1.0000000504$. The corrections $a_n^{(2)}$ and $a_n^{(4)}$ approach their large-n asymptotical behavior, $-2A_{n+1}$ and $2/3A_{n+2}$ with a slower rate. For comparison, $\frac{a_{3499}^{(2)}}{-2A_{3500}} = 0.999647$ and $\frac{a_{3500}^{(4)}}{2\,/\,3A_{3502}} = 0.99789$.

built based on the first several coefficients of the series is known as a generalized summation method. A popular approach in theoretical physics is the method of Padé approximants [30]. The Padé approximant $[M, N]$ to the power series $F(\lambda) = \sum_{k=0}^{\infty} b_k \lambda^k$ is defined as a solution of the linear equation $A\tilde{F} + B = 0$, where A and B are polynomials of degrees M and N such that $AF + B = o(\lambda^{M+N})$.

Along with Padé approximants, we consider a generalization of Padé approximants known as algebraic, or Padé–Hermite approximants [31]. A quadratic Padé approximant $[L, M, N]$ is defined as a solution of the quadratic equation $A\tilde{F}^2 + B\tilde{F} + C = 0$, where polynomials A, B, and C, of degrees L, M, and N respectively, are defined such that $AF^2 + BF + C = o(\lambda^{L+M+N+1})$. Generally, algebraic approximants are solutions of an algebraic equation of m-th degree and approximate the function by m branches of an analytic function. The main branch usually coincides with the result of common summation. Secondary branches represent the result of 'analytic extension', i.e. the analytic continuation of the power series along a complex path that may go around branch points. For example, the summation of the power series for logarithmic function $\log(1 + \lambda) = \lambda - \lambda^2/2 + \lambda^3/3 - \lambda^4/4 + \ldots$ gives the result $\log(1 + \lambda)$ in the main branch and supplementary complex-valued branches $\log(1 + \lambda) + 2\pi k\mathrm{i}$ for non-zero integer k in secondary branches [32]. The method of complex extension was used previously, for example, to derive a semiclassical approximation for resonant (quasi-stationary) states of atomic and molecular systems by extending the bound state energies expanded around a minimum of a potential to the case when the potential does not have minima, but has only complex-valued stationary points [33]. In the same paper, the authors used quadratic Padé approximants to recover the complex-valued resonance energies in the case that the minimum of the potential exists, and the series is purely real. For the quantum anharmonic oscillator, any eigenvalue could be in principle obtained by analytic continuation of a single fixed eigenvalue over a coupling constant [34]. We show here that algebraic approximants appear to be a powerful tool to

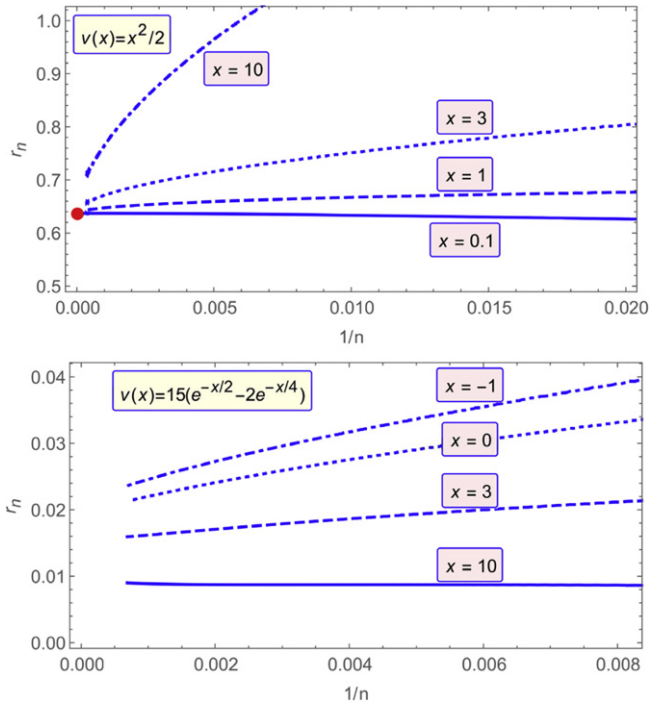

Figure 6. Convergence of the ratios r_n given by equation (23) to the large-n limit equal to the inverse radius of convergence $1/R$ for different values of the coordinate x. The upper panel is the Borel transform of the series for harmonic oscillator, and the lower panel is the generalized Borel transform (given by equation (24) for the Morse potential. On the upper panel, a large dot marks the inverse radius of convergence at $x = 0$ equal to $2/\pi$. Apparently, the sequence of ratios converges to this limit for all given values of x. For the Morse potential, different curves converge to different limits, that indicates that the radius of convergence depends on the coordinate x.

connect a function described by the gradient expansion and the real electronic density into a single analytic function.

Recalling that the function $F(\lambda)$ is defined as the sum in equation (10), we have

$$\rho = \frac{p_{\mathrm{F}}}{\pi} F(\lambda). \tag{25}$$

At first glance, it would be tempting to apply Padé approximants to the series (10) directly. It is possible in principle, but it has several disadvantages. Firstly, we notice that ρ as a function of the coordinate x does not have singularities, while p_{F} has square-root singularities at turning points. Therefore, $F(\lambda)$ has square-root singularities at turning points too. We may consider summation of the series for $F^2(\lambda)$ instead of $F(\lambda)$, expecting that the rational-type approximants are better suited to simple pole singularities. Secondly, we are going to employ a fast algorithm for calculation of Padé approximants [35]. This algorithm fails in special cases when either b_0 or b_1 are zero. Since in our case $b_1 = 0$, it would be desirable to approximate the series $\sum_{n=0}^{\infty} b_{n+2}\lambda^n$ instead of the original series (10), as all the coefficients starting from b_2 are non-zero (here we do not consider a special case of $x = 0$, when all odd-order coefficients vanish). By taking into account these two considerations, we choose to apply the approximants to the series

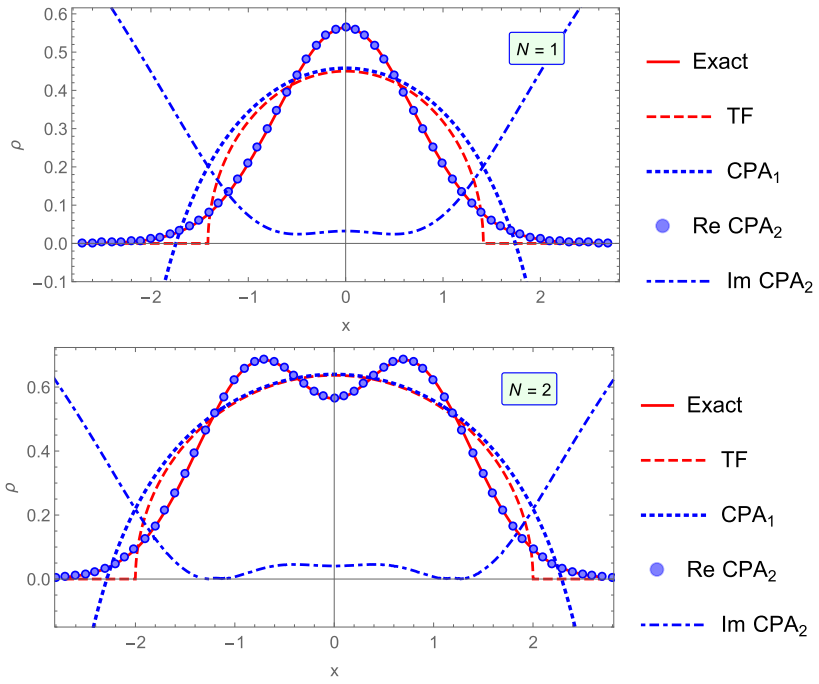

Figure 7. Thomas–Fermi (dashed) and exact density (solid) of one and two particles in the harmonic potential, $v(x) = x^2/2$. Dots are results of summation of the series (17) in the main branch using algebraic approximants of degree $m = 3$. It is a bell-shaped curve without oscillations. A real part of the complex-valued branch shown by circles coincides with the exact density (solid curve). The imaginary part of this result is shown too, a dot-dashed curve.

$$\tilde{F}(\lambda) = \sum_{n=0}^{\infty} \tilde{b}_n \lambda^n, \quad \tilde{b}_n = \sum_{m=0}^{n+2} b_n b_{n-m+2}, \tag{26}$$

so that the original function F can be recovered from the approximation $\tilde{F}$ as $F = (1 + \lambda^2 \tilde{F})^{1/2}$.

Our first attempt to sum the series is calculation of a 'staircase' sequence of Padé approximants, [0, 0], [0, 1], [1, 1], [1, 2], [2, 2], …, for the harmonic oscillator. The results for a typical case of $x = 1$ are shown in table 3. The order of the approximant $[n_1, n_2]$ is defined as $n = n_1 + n_2$. It appears that the traditional Padé approximants do not approach a certain limit as n increases. Then, we attempt to use the quadratic Padé approximants. One of branches of the quadratic approximants seems to converge to a certain limit which is close to the Thomas–Fermi density (numerically, the limit is 0.343377 versus 0.31831 for the Thomas–Fermi density, at $N = 1$ and $x = 1$). Finally, we attempt to use cubic approximants. They are labeled by four integers $[n_1, n_2, n_3, n_4]$ which are degrees of the corresponding polynomials. We assume here that $n_1 \leqslant n_2 \leqslant n_3 \leqslant n_4 \leqslant n_1 + 1$, so that these numbers are uniquely defined by the order of the approximant $n = n_1 + n_2 + n_3 + n_4 + 2$. Table 3 shows that all branches of the cubic approximants converge to certain limits, one of them is real and coincides with the limit of quadratic approximants, and the other two are complex-conjugate. Notice that the real part of the complex-valued branch approaches the exact

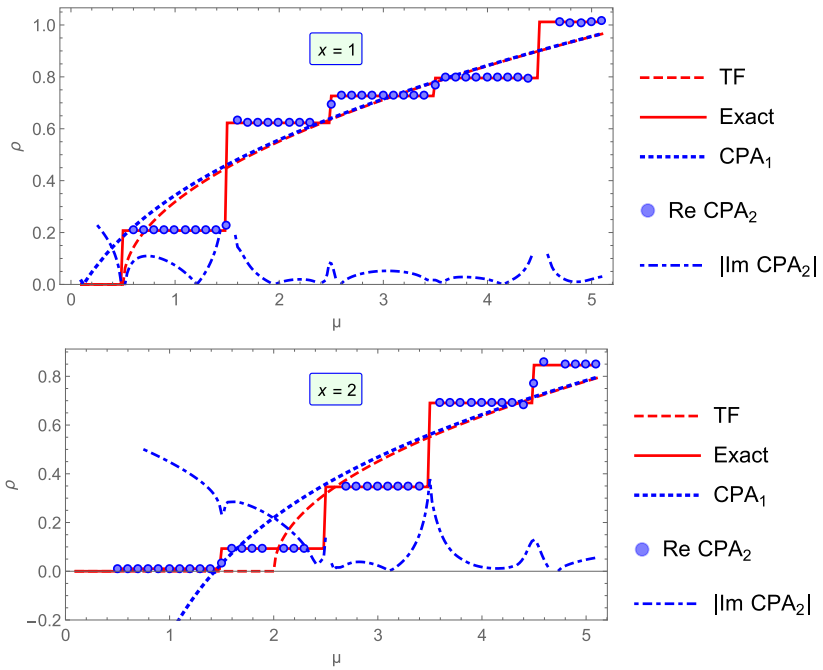

Figure 8. Dependence of results of summation of the gradient expansion on the chemical potential μ, for two different values of the coordinate x. If the chemical potential varies between two successive eigenvalues of the harmonic oscillator (half-integer numbers), then the result of summation (in real part) does not change and equates to the exact density (stepwise solid curve). For comparison, Thomas–Fermi (dashed curve), the result of summation in the real branch (dotted curve), and the imaginary part of the complex-valued branch (dot-dashed curve) are shown too.

density. We did not anticipate in advance this numerical coincidence and up to now we do not have any supporting arguments apart from numerical results.

We found that for a high-order cubic approximant one of the branches is purely real, and two other branches are complex-conjugate. We call the real branch the main branch, because it is close to the results of ordinary summation in the case when coordinate x is small and when the ordinary summation converges in low orders. The main branch for number of particles equal to one and two is shown on figure 7. The main branch does not reproduce either oscillations or the exponential tail of the density in the classically forbidden region. Real and imaginary parts of two other branches of the cubic approximants are shown on figure 7 too.

Above, we have always used the same chemical potential $\mu = N$ that gives correct normalization for the Thomas–Fermi density. It would be interesting to check how the result of summation changes with variation of μ. We found that small variations (less than $1/2$ in magnitude, when μ does not cross any eigenvalues of the harmonic oscillator, $n + 1/2, \quad n = 0, 1, 2, \ldots$) do not change the real part of the complex-valued branches, so this real part always coincides with the exact density, while the imaginary part as well as the real branch change with μ. The dependence on μ is shown on figure 8.

For calculation of algebraic approximants, we used a recursive algorithm [35]. Since it is numerically unstable, we used multiple precision arithmetic.

6. Conclusion

We consider here electronic density for a bound system and its gradient expansion within the frame of potential functional theory, for a given potential in one dimension. We try to answer two questions, (1) whether the gradient expansion represents an asymptotic series to the density and (2) whether the gradient expansion is a convergent series and if it can be summed, then what is the relation between the sum of the series and the density. While the answer to the first question is negative because of the presence of quantum oscillations in the density that are missing in the first semiclassical correction to the leading term (Thomas–Fermi approximation) in the gradient expansion, we demonstrate numerically that the asymptotical behavior of the gradient expansion is restored after smoothing the oscillations in the density. Regarding summation of the gradient expansion we show that the series is always divergent, even in the semiclassical region of large quantum numbers, because of the factorial growth of its coefficients. Using cubic Padé approximants, we obtained in the limit of large orders a convergent result which is a real function along with a pair of complex-conjugate functions that together form three different branches of a single multiple-valued function that is a solution of the cubic equation. Interestingly, the real part of the complex-valued branches precisely coincides with the oscillating density, while the real branch is close to the Thomas–Fermi density and does not show oscillations. Thus, the density can in principle be restored from information contained in several first terms of the gradient expansion, even though in practice the required number of terms could be very large. These numerical experiments reveal previously unknown aspects of the theory that allow one to use it even in the presence of oscillations and turning points where the gradient expansion is commonly considered as inapplicable.

References

[1] Yang W, Ayers P W and Wu Q 2004 *Phys. Rev. Lett.* **92** 146404
[2] Cangi A, Lee D, Elliott P, Burke K and Gross E K U 2011 *Phys. Rev. Lett.* **106** 236404
[3] Peng D G, Zhao B, Cohen A J, Hu X Q and Yang W T 2012 *Mol. Phys.* **110** 925–34
[4] Cangi A, Gross E K U and Burke K 2013 *Phys. Rev.* A **88** 14
[5] Holas A and March N H 1995 *Phys. Rev.* A **51** 2040
[6] March N H and Plaskett J S 1956 *Philos. Trans. Roy. Soc. London Ser.* A **235** 419–31
[7] Brack M, Jennings B K and Chu Y H 1976 *Phys. Lett.* B **65** 1–4
[8] Conlon J G 1983 *J. Math. Phys.* **24** 184
[9] Lieb E H and Simon B 1977 *Adv. Math. (NY)* **23** 22–116
[10] Benguria R and Lieb E H 1978 *Ann. Phys. (NY)* **110** 34–45
[11] Lieb E H 1981 *Rev. Mod. Phys.* **53** 603
[12] March N H 1981 *Phys. Chem. Liq.* **48** 141–55
[13] Sergeev A, Jovanovic R, Kais S and Alharbi F H 2015 *Phys. Scr.* **90** 125401
[14] Murphy D R 1981 *Phys. Rev.* A **24** 1682–8
[15] Yan Z D, Perdew J P, Korhonen T and Ziesche P 1997 *Phys. Rev.* A **55** 4601–4
[16] Ribeiro R F, Lee D, Cangi A, Elliott P and Burke K 2015 *Phys. Rev. Lett.* **114** 050401
[17] Samaj L and Percus J K 1999 *J. Chem. Phys.* **111** 1809–14
[18] Elliott P, Lee D, Cangi A and Burke K 2008 *Phys. Rev. Lett.* **100** 256406
[19] Cangi A, Lee D, Elliott P and Burke K 2010 *Phys. Rev.* B **81** 14
[20] Alonso J A and Girifalco L A 1978 *Chem. Phys. Lett.* **53** 190–1
[21] Murphy D R and Parr R G 1979 *Chem. Phys. Lett.* **60** 377–9
[22] Bender C M and Orszag S A 1999 *Advanced Mathematical Methods for Scientists and Engineers* (New York: Springer-Verlag)
[23] Loeffel J J, Martin A, Simon B and Whiteman A S 1969 *Phys. Lett.* B **30** 656–8
[24] Graffi S, Grecchi V and Turchetti G 1970 *Nuovo Cimento Soc. Ital. Fis.* B **4** 313–40
[25] Dyson F J 1952 *Phys. Rev.* **85** 631–2

[26] Bender C M and Wu T T 1969 *Phys. Rev.* **184** 1231–60
[27] Mercer G N and Roberts A J 1990 *SIAM J. Appl. Math.* **50** 1547–65
[28] Hardy G H 1949 *Divergent Series* (Oxford: Clarendon Press)
[29] Arteca G A, Fernández F M and Castro E A 1990 Large order perturbation theory and summation methods in quantum mechanics *Lecture Notes in Chemistry* 53 (New York: Springer-Verlag)
[30] Baker G A and Gammel J L (ed) 1970 *The Padé Approximants in Theoretical Physics* (New York: Academic Press)
[31] Boyd J P and Natarov A 2002 *Appl. Math. Comput.* **126** 109–17
[32] Sergeev A V and Goodson D Z 1998 *J. Phys. A: Math. Gen.* **31** 4301
[33] Germann T C and Kais S 1993 *J. Chem. Phys.* **99** 7739
[34] Simon B 1970 *Ann. Phys.* **58** 76–136
[35] Sergeev A 1986 *U. S. S. R. Comput. Maths. Math. Phys.* **26** 17